Light-Induced Pulling and Pushing by the Synergic Effect of Optical Force and Photophoretic Force

Jinsheng Lu, Hangbo Yang, Lina Zhou, Yuanqing Yang, Si Luo, Qiang Li, and Min Qiu*
State Key Laboratory of Modern Optical Instrumentation, College of Optical Science and Engineering, Zhejiang University, 310027 Hangzhou, China
(Received 21 September 2016; published 23 January 2017)

Optical force, coming from momentum exchange during light-matter interactions, has been widely utilized to manipulate microscopic objects, though mostly in vacuum or in liquids. By contrast, due to the light-induced thermal effect, photophoretic force provides an alternative and effective way to transport light-absorbing particles in ambient gases. However, in most cases these forces work independently. Here, by employing the synergy of optical force and photophoretic force, we propose and experimentally demonstrate a configuration which can drive a micron-size metallic plate moving back and forth on a tapered fiber with supercontinuum light in ambient air. Optical pulling and oscillation of the metallic plate are experimentally realized. The results might open exhilarating possibilities in applications of optical driving and energy conversion.

DOI: 10.1103/PhysRevLett.118.043601

Light-induced forces stem from momentum transfer directly between photons and objects, or indirectly between surrounding media and objects when light interacts with objects. The force that comes from the direct way is the well-known optical force, which has been widely used to manipulate microscopic objects in the fields of physics, biochemistry, and clinical medicine [1–9]. Photophoretic force, originating from the indirect way with the light-induced thermal effect, provides an alternative and effective way to transport light-absorbing particles in ambient gases [10–14]. Recently, light-induced pulling is of significant interest since it provides a new understanding of the light-matter interaction [12,15]. Pulling force can be achieved by different methods [16] including using optical gradient force [17–19], enhancing forward scattering of the object [15,20–23], utilizing mode coupling between the object and a waveguide [24,25], or exploiting enhancement of light momentum at dielectric interface [26], all known as *optical* pulling force. Among these methods, attracting dielectric objects (usually treated as nonabsorbing objects) against the field propagation has been shown experimentally with the help of optical pulling force [17,22,26,27], though all in liquids.

For light-absorbing objects in gases, when the absorption predominantly happens in the front part of the object in the direction along the light propagation, the temperature in the front part of the object will be higher than that of the back-end part, causing a greater energy being transferred to the surrounding gas near the front part of the object [28]. Then the gas molecules near the front part of the object will impart a larger force in a direction opposite the light propagation to the object. Since the force imparted by the gas molecules can be far larger than the force coming from photon momentum being transferred to the object during the absorption [29], this temperature difference will result in a pulling force on the object. This light-induced pulling force, which is termed as *photophoretic* pulling force, provides a more effective way to attract absorbing particles in ambient gases [12,13]. It is worth noting that the photophoretic forces are usually neglected for manipulating objects in liquids due to sufficiently high thermal conductivity of the liquids (e.g., water).

Optical forces and photophoretic forces are usually used to manipulate objects independently in most cases, as working in different environments. Only very few works discuss that these two kinds of forces work together to control objects [30]. Moreover, most previous research achieves pulling force using free space beams [12,13,17,22,26,27] in their experiments, which is limited by the diffraction and lacks the flexibility in moving and focusing. In this regard, using an easily fabricated and flexible tapered fiber as an optical driving tool would be an excellent alternative [31].

Here we propose and experimentally demonstrate a way to realize the light-induced pulling and pushing of a gold plate using a tapered fiber guided with supercontinuum light in ambient air. We show that a micrometer-sized gold plate can be pulled against the direction of light propagation from the tapered fiber end by a strong photophoretic pulling force together with a weak optical pulling force. The gold plate can then be pushed back by an optical pushing force. Thus, we can optically drive the gold plate back and forth on the tapered fiber with a speed up to 28 μm/s.

The schematic of the driving system in Figs. 1(a), 1(b) describes a gold plate (side length, 5.4 μm; thickness, 30 nm) being pulled from the tapered fiber end (cone angle, 6°), and then pushed back after the gold plate is pulled to

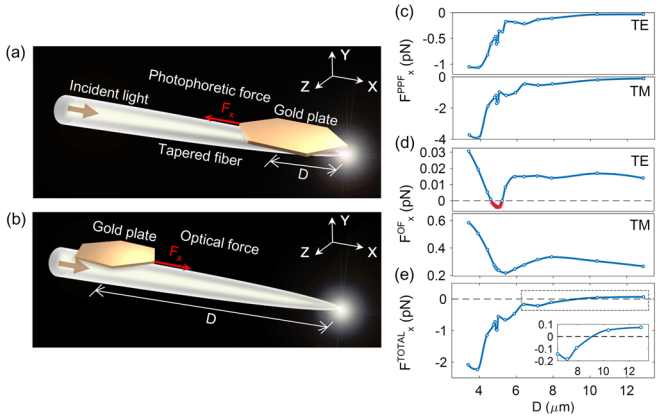

FIG. 1. Numerical modeling of light-induced driving by synergy effect of optical force and photophoretic force. (a),(b) Schematic of pulling a hexagonal gold plate (side length, 5.4 μm; thickness, 30 nm) up on a tapered fiber (cone angle, 6°) near the tapered fiber end (a) and pushing the same gold plate back in the middle section of the tapered fiber (b) in ambient air. The tapered fiber is guided with unpolarized supercontinuum light (power, 1.3 mW). The distance between the center of the gold plate and the tapered fiber end is D. (c),(d),(e) Calculated (c) photophoretic force (F_x^{PPF}), (d) optical force (F_x^{OF}), and (e) total light-induced force (F_x^{TOTAL}) along the tapered fiber acting on the gold plate. The inset in (e) shows an enlarged view of the part enclosed by the dashed box. The total light-induced force is calculated with the sum of the optical force and the photophoretic force, and both the TE and TM mode account for 50 percent. The red curve in (d) represents regions with optical pulling force ($F_x^{\mathrm{OF}} < 0$). Non-zero electromagnetic field components are E_z, H_x, H_y for the TE mode and E_x, E_y, H_z for the TM mode. Here, we use the piecewise cubic hermite interpolating polynomial (PCHIP) to connect the data points with a smooth curve.

the middle section of the tapered fiber. Let us first investigate the force coming from the light-induced thermal effect, i.e., a photophoretic force. The temperature distribution of the gold plate in the y direction is almost the same due to the small thickness (30 nm) and the high thermal conductivity of the gold. However, the temperature distribution in the gold plate is not uniform along the x direction (as shown in the thermal simulation results in Fig. S4 in the Supplemental Material [32]). The temperature in the front part of the gold plate is higher than that of the back-end part, especially when the gold plate is near the tapered fiber end. When the gold plate is at a location away from the tapered fiber end, the temperature difference then goes to zero. This temperature difference change can be interpreted by the different electromagnetic field distribution along the tapered fiber. The diameter of the fiber becomes smaller towards the fiber end, and the evanescent field outside of the fiber becomes stronger, especially at the tapered fiber end, making a more efficient light-induced heat source in the front part of the gold plate due to the absorption. The large temperature difference when the gold plate is near the tapered fiber end would induce a large photophoretic pulling force. The photophoretic force of a thin plate in the continuum regime comes mostly from the thermal creep force, which can be estimated as [43] $F^{\mathrm{PPF}} = -15/(64\sqrt{2})k_B/\sigma_{\mathrm{cs}}\alpha dT/dxS_v$, where, k_B is Boltzmann's constant, σ_{cs} is the scattering cross section of gas molecules, α is the thermal accommodation coefficient, dT/dx is the temperature gradient across the plate, and S_v is the area of the surface parallel to the temperature gradient of the thin plate. The calculated photophoretic forces are shown in Fig. 1(c) (see calculation details in the Supplemental Material [32], Sec. IV). The photophoretic force is always negative (i.e., a photophoretic pulling force) in this configuration. When the gold plate is at a location far away from the tapered fiber end, the photophoretic force goes to zero.

Now let us study the optical forces coming from light scattering. The calculated results for optical force are shown in Fig. 1(d). The supercontinuum light induced optical force is derived from the overlap integral between single-wavelength light-induced optical force spectrum and light source power density spectrum (see Supplemental Material [32], Sec. III for detailed calculation methods). Different from the photophoretic force serving mostly as a pulling force, optical force mainly acts as a pushing force along the tapered fiber (i.e., along the x direction). Surprisingly, there also exists a weaker optical pulling force ($F_x^{\mathrm{OF}} < 0$) when D is around 4.9 μm and the guided mode in the tapered fiber is the transverse electric (TE) mode. As for the optical force in the y direction (between the gold plate and the tapered fiber), it is a repulsive force ($F_y^{\mathrm{OF}} > 0$) for TE mode and an attractive force ($F_y^{\mathrm{OF}} < 0$) for transverse magnetic (TM) mode (see Fig. S8).

The total light-induced force along the tapered fiber is the sum of the optical force F_x^{OF} and the photophoretic force F_x^{PPF} as shown in Fig. 1(e). Since the photophoretic force is far larger than the optical force near the tapered fiber end, the total light-induced force near the tapered fiber is negative (i.e., pulling the gold plate away from the tapered fiber end). When the gold plate is pulled to a location away from the tapered fiber end, the photophoretic force will go to zero while the optical force is still positive, so the total force becomes positive (i.e., pushing the gold plate back to the tapered fiber end).

The above discussions are confirmed experimentally. The unpolarized supercontinuum light is delivered into a tapered fiber (cone angle, 6°) as illustrated in Fig. 2. The micrometer-sized gold plates are deposited on the glass substrate and then dried. The tapered fiber is manipulated by the three-dimensional console to pick up the gold plate in ambient air (see Supplemental Material [32], Sec. II). The effect of light-induced pulling and pushing is shown in Fig. 3. Figure 3 presents sequencing images of the gold plate being pulled and pushed by a tapered fiber guided with supercontinuum light in ambient air. The gold plate (side length, 5.4 μm; thickness, 30 nm) is placed on the tapered fiber end. After the supercontinuum light being guided into the tapered fiber

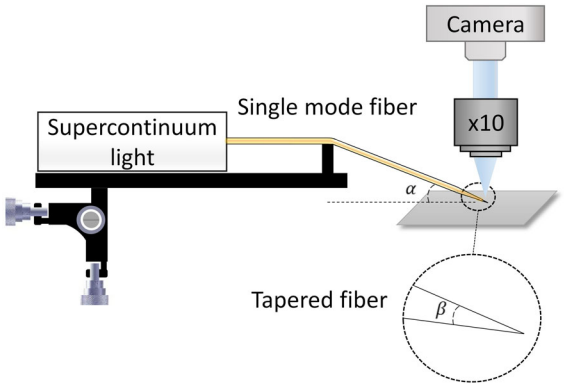

FIG. 2. Experimental configuration. The supercontinuum light is delivered into a single mode fiber connected with a tapered fiber. The optical microscope including a 10× microscope objective, and a camera is used for observation. The tapered fiber is slightly tilted down (α) around 9° and the cone angle (β) of the tapered fiber is about 6°. The tapered fiber is mounted on a three dimensional console and suspended in ambient air.

(power, 1.3 mW), the gold plate is pulled back at an average speed of 35.6 μm/s at first, next, it is pushed forward at an average speed of 28.52 μm/s, thereafter, it is pulled back again at an average speed of 37.11 μm/s, and finally, it stops in a location 43 μm away from the tapered fiber end (see real-time movie in Supplemental Material [32], video 1).

It is worth noting that the back and forth movement of a gold plate happens only when the initial position of the plate is away from the tapered fiber end, i.e., $D > 5.5$ μm, where the total pushing force (positive) is comparable to the total pulling force (negative), as seen in the inset of Fig. 1(e). If a gold plate is placed on the tapered fiber near the end (i.e., $D < 4.4$ μm), the very large pulling force can pull the gold

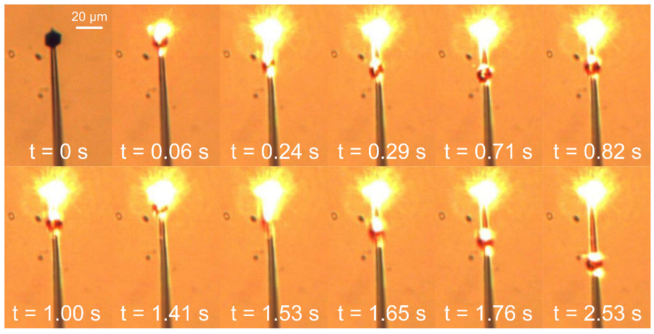

FIG. 3. Sequencing optical microscopy images of a back-and-forth moving gold plate driven by unpolarized supercontinuum light on a tapered fiber in ambient air. The cone angle of tapered fiber used in experiment is about 6°. A time series of images shows that the gold plate is first pulled backward at an average speed of 35.60 μm/s after the light is switched on, next, it is pushed forward at an average speed of 28.52 μm/s, thereafter, it is pulled back again at an average speed of 37.11 μm/s, and finally, it stops at a location 43 μm away from the tapered fiber end (see Supplemental Material [32], video 1). The total power of supercontinuum light guided into the tapered fiber is 1.3 mW.

plate to a location so far away from the tapered fiber end that the gold plate stops there and cannot be pushed back again. This is due to the fact that the small pushing force (F_x^{OF}) from the weak evanescent field cannot offset the large friction force between the gold plate and the tapered fiber, causing the gold plate to stop moving. This is also observed in our experiments, where the gold plate is pulled against the direction of light propagation up to 80 μm from the tapered fiber end at first and stops there finally (see real-time movie in Supplemental Material [32], video 2).

The wavelength dependence of the optical force and the photophoretic force are also investigated and shown in Fig. 4. Though the optical pulling force is fairly weak in our configuration, interestingly, the optical pulling force exists in a broadband nearly 1000 nm of wavelength from 450 to 1450 nm as seen in Fig. 4(a) for the TE mode. We find that the optical pulling force in this configuration originates from the phase difference shift (from π to 0) of the magnetic components (H_x and H_y) at the tapered fiber end (see Supplemental Material [32], Sec. V).

In conclusion, we have shown that optical force and photophoretic force can be used synergistically to drive a gold plate moving back and forth on a tapered fiber. A light-induced oscillation of the gold plate is experimentally realized on a tapered fiber. The extremely simple and flexible configuration can be easily implemented on compact lab-on-a-chip systems. Such light-induced driving systems could further serve to promote extensive applications in many fields of fundamental science and technology, of which typical examples include energy conversion from light energy to mechanical energy. Our studies could offer a

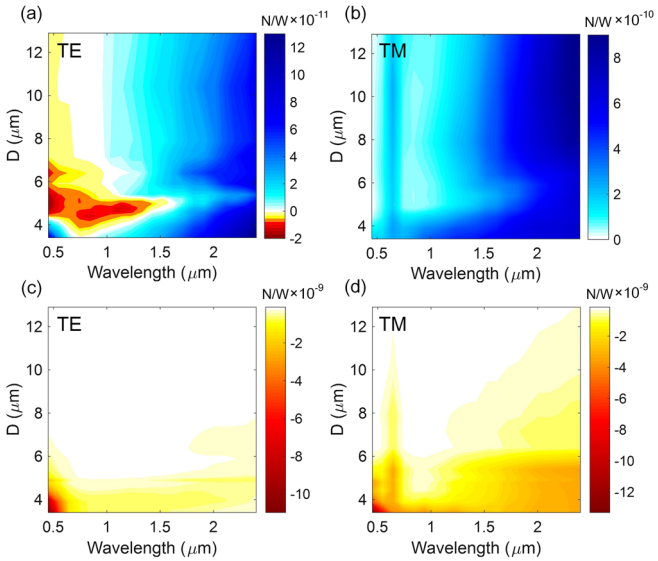

FIG. 4. Calculated optical force (F_x^{OF}) and photophoretic force (F_x^{PPF}) with respect to the wavelength of light source and the distance (D) between the center of gold plate and the tapered fiber end. (a),(b) Optical force.(c), (d) Photophoretic force. (a), (c) TE mode. (b), (d) TM mode.

deeper understanding of a diversified light-matter interaction, opening up new avenues for pluralistic optical manipulation including optical control and sensing, and inspiring various research on optical driving (e.g., light-driven motor).

This work is supported by the National Natural Science Foundation of China (Grants No. 61425023, No. 61575177, and No. 61235007).

*minqiu@zju.edu.cn

[1] W. D. Phillips, Rev. Mod. Phys. **70**, 721 (1998).
[2] T. L. Min, P. J. Mears, L. M. Chubiz, C. V. Rao, I. Golding, and Y. R. Chemla, Nat. Methods **6**, 831 (2009).
[3] E. Eriksson, K. Sott, F. Lundqvist, M. Sveningsson, J. Scrimgeour, D. Hanstorp, M. Goksör, and A. Granéli, Lab Chip **10**, 617 (2010).
[4] A. N. Grigorenko, N. W. Roberts, M. R. Dickinson, and Y. Zhang, Nat. Photonics **2**, 365 (2008).
[5] M. A. Taylor, M. Waleed, A. B. Stilgoe, H. Rubinsztein-Dunlop, and W. P. Bowen, Nat. Photonics **9**, 669 (2015).
[6] M. Liu, T. Zentgraf, Y. M. Liu, G. Bartal, and X. Zhang, Nat. Nanotechnol. **5**, 570 (2010).
[7] J. H. Kang, K. Kim, H. S. Ee, Y. H. Lee, T. Y. Yoon, M. K. Seo, and H. G. Park, Nat. Commun. **2**, 582 (2011).
[8] K. Wang, E. Schonbrun, P. Steinvurzel, and K. B. Crozier, Nat. Commun. **2**, 469 (2011).
[9] M. C. Zhong, X. B. Wei, J. H. Zhou, Z. Q. Wang, and Y. M. Li, Nat. Commun. **4**, 1768 (2013).
[10] H. Rohatschek, J. Aerosol Sci. **26**, 717 (1995).
[11] G. Wurm and O. Krauss, Phys. Rev. Lett. **96**, 134301 (2006).
[12] V. Shvedov, A. R. Davoyan, C. Hnatovsky, N. Engheta, and W. Krolikowski, Nat. Photonics **8**, 846 (2014).
[13] J. Lin, A. G. Hart, and Y. Q. Li, Appl. Phys. Lett. **106**, 171906 (2015).
[14] V. G. Shvedov, A. V. Rode, Y. V. Izdebskaya, A. S. Desyatnikov, W. Krolikowski, and Y. S. Kivshar, Phys. Rev. Lett. **105**, 118103 (2010).
[15] J. Chen, J. Ng, Z. F. Lin, and C. T. Chan, Nat. Photonics **5**, 531 (2011).
[16] A. Dogariu, S. Sukhov, and J. J. Saenz, Nat. Photonics **7**, 24 (2013).
[17] S-H. Lee, Y. Roichman, and D. G. Grier, Opt. Express **18**, 6988 (2010).
[18] A. A. Bogdanov, A. S. Shalin, and P. Ginzburg, Sci. Rep. **5**, 15846 (2015).
[19] A. S. Shalin, S. V. Sukhov, A. A. Bogdanov, P. A. Belov, and P. Ginzburg, Phys. Rev. A **91**, 063830 (2015).
[20] A. Novitsky, C. W. Qiu, and H. F. Wang, Phys. Rev. Lett. **107**, 203601 (2011).
[21] S. Sukhov and A. Dogariu, Phys. Rev. Lett. **107**, 203602 (2011).
[22] O. Brzobohatý, V. Karásek, M. Šiler, L. Chvátal, T. Čižmár, and P. Zemánek, Nat. Photonics **7**, 123 (2013).
[23] M. I. Petrov, S. V. Sukhov, A. A. Bogdanov, A. S. Shalin, and A. Dogariu, Laser Photonics Rev. **10**, 116 (2016).
[24] V. Intaraprasonk and S. H. Fan, Opt. Lett. **38**, 3264 (2013).
[25] A. V. Maslov, Phys. Rev. Lett. **112**, 113903 (2014).
[26] V. Kajorndejnukul, W. Q. Ding, S. Sukhov, C. W. Qiu, and A. Dogariu, Nat. Photonics **7**, 787 (2013).
[27] D. B. Ruffner and D. G. Grier, Phys. Rev. Lett. **109**, 163903 (2012).
[28] Y. I. Yalamov, V. B. Kutukov, and E. R. Shchukin, J. Colloid Interface Sci. **57**, 564 (1976).
[29] G. M. Hidy and J. R. Brock, J. Geophys. Res. **72**, 455 (1967).
[30] O. A. Schmidt, M. K. Garbos, T. G. Euser, and P. S. J. Russell, Phys. Rev. Lett. **109**, 024502 (2012).
[31] H. B. Xin, R. Xu, and B. J. Li, Sci. Rep. **2**, 818 (2012).
[32] See Supplemental Material at http://link.aps.org/supplemental/10.1103/PhysRevLett.118.043601 for additional detailed experimental procedures, numerical calculation methods, and physical mechanisms of the optical pulling force, which includes Refs. [33–42].
[33] L. Tong, R. R. Gattass, J. B. Ashcom, S. He, J. Lou, M. Shen, I. Maxwell, and E. Mazur, Nature (London) **426**, 816 (2003).
[34] Z. Guo, Y. Zhang, Y. DuanMu, L. Xu, S. Xie, and N. Gu, Colloids Surf. A **278**, 33 (2006).
[35] L. Novotny and B. Hecht, *Principles of Nano-Optics* (Academic, Cambridge, 2012), Chap. 13.
[36] K. Wang, E. Schonbrun, and K. B. Crozier, Nano Lett. **9**, 2623 (2009).
[37] C. Min, Z. Shen, J. Shen, Y. Zhang, H. Fang, G. Yuan, L. Du, S. Zhu, T. Lei, and X. Yuan, Nat. Commun. **4**, 2891 (2013).
[38] X. Chen, Y. T. Chen, M. Yan, and M. Qiu, ACS Nano **6**, 2550 (2012).
[39] D. Wolfe, A. Larraza, and A. Garcia, Phys. Fluids **28**, 037103 (2016).
[40] M. Scandurra, arXiv:physics/0402011.
[41] Yinshun Wang, *Fundamental Elements of Applied Superconductivity in Electrical Engineering* (John Wiley & Sons, New York, 2013), Chap. 9.
[42] S. Gaugiran, S. Gétin, J. M. Fedeli, and J. Derouard, Opt. Express **15**, 8146 (2007).
[43] M. Scandurra, F. Iacopetti, and P. Colona, Phys. Rev. E **75**, 026308 (2007).